SPECTROSCOPIC ANALYSIS OF SDB BINARIES FROM THE SPY PROJECT

C. Karl[1], U. Heber[1], R. Napiwotzki[2] and S. Geier[1]

[1] *Remeis-Sternwarte, Sternwartstrasse 7, D-96049 Bamberg, Germany*

[2] *Centre for Astrophysics Research, University of Hertfordshire, College Lane, Hatfield AL10 9AB, U.K.*

Abstract. In the course of our search for double degenerate binaries as potential progenitors of type Ia supernovae with the ESO VLT several new subdwarf B (sdB) binaries were discovered. In this paper, we present detailed analysis of six radial velocity variable sdB stars. Radial velocity curves have been measured. From the mass functions we derive lower limits to the masses of the unseen companions and discuss their nature. In addition, effective temperatures, surface gravities, helium abundances and metal abundances were determined.

Key words: binaries: spectroscopic – stars: atmospheres – stars: hot subdwarfs

1. INTRODUCTION

There is a general consensus that the precursors of type Ia supernovae (SN Ia) are white dwarfs in close binary systems. These white dwarfs accrete matter from their companions until a critical mass limit is reached. The two scenarios for SN Ia formation differ in the nature of the companion. This is a main-sequence or red giant star in the so-called 'single degenerate' scenario, and is another white dwarf in the 'double degenerate' scenario.

The purpose of the 'Supernova Ia progenitor survey' (SPY) was to check the double degenerate scenario by observational means. Thus, we observed more than 1000 WDs over the course of four years at the ESO VLT equipped with UVES in order to check the objects for radial velocity (RV) variations (cf. Napiwotzki et al. 2003). Follow-up observations of promising objects were performed in order to derive system parameters like periods (P) and RV semi-amplitudes (K). In combination with quantitative spectral analyses we computed the systems' total masses and merging times. A very promising SN Ia precursor candidate was discovered by Napiwotzki et al. (2005) in the course of our project.

Due to mis-classification in the input catalogue the SPY sample also contains a number of subdwarf B stars (sdBs; Lisker et al. 2005). Since these objects are immediate precursors of white dwarfs, they are also promising objects with respect to the search for SN Ia progenitors. For example, Maxted et al. (2000) and Geier et al. (2006) found the sdB binary KPD 1930+2752 to be a SN Ia
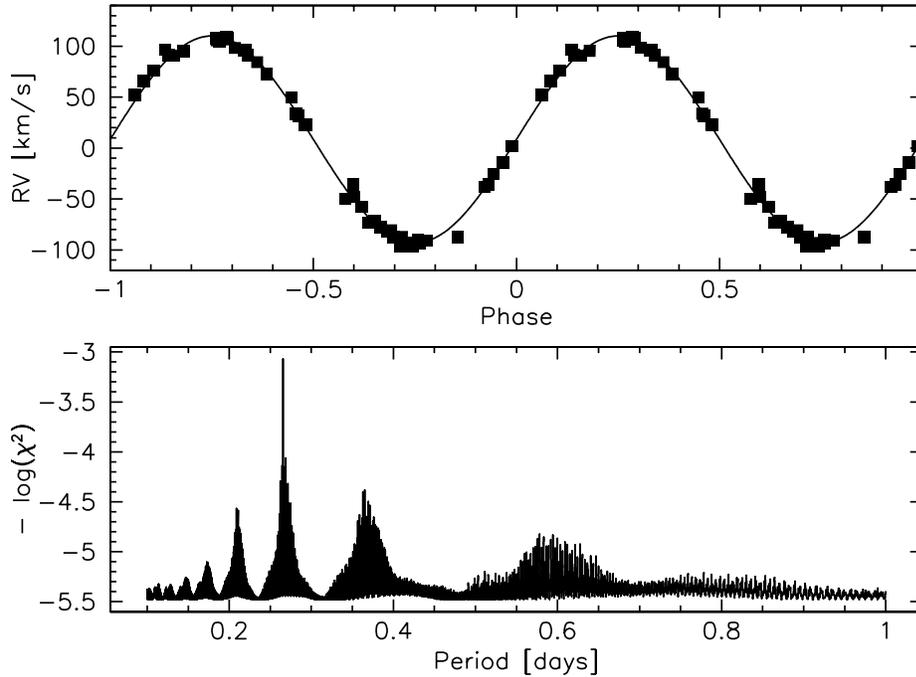
Fig. 1. Sample best fit RV curve and power spectrum for the visible sdB star in the HE 0532-4503 system. Upper panel: measured radial velocities as a function of orbital phase and fitted sine curve. Lower panel: power spectrum.

precursor candidate. Thus promising RV variable sdB stars were included in our follow-up observations as well.

In this paper we present the results of an analysis of six sdB binaries discovered by SPY.

2. OBSERVATIONS AND RADIAL VELOCITY CURVES

All program stars were observed at least twice in the course of the SPY project at the ESO VLT. Additional observations were made during follow-up campaigns at the ESO NTT (equipped with EMMI), the ESO VLT (UVES), the Calar Alto Observatory 3.5 m telescope (TWIN) and the 4 m WHT (ISIS) at La Palma.

Radial velocities of the individual observations are determined by calculating the shifts of the measured wavelengths relative to their laboratory values. Since the S/N ratio was of the order of 15 to 30, most of the narrow metal lines were hardly visible in our individual spectra. We therefore focussed on all available He I lines and on the observed Hα line profile because of its sharp and well-defined non-LTE line core. We performed a simultaneous fit of a set of mathematical functions to the observed line profiles using the ESO MIDAS package. A linear function was used to reproduce the overall spectral trend and a Gaussian for the innermost line core. In order to fit the Hα profile we used an additional Lorentzian to model the broad line wings. The central wavelength of the Lorentzian was fixed to that of the Gaussian for physical reasons.

The period search was carried out by means of a periodogram based on the 'Singular Value Decomposition' method. For a large range of periods the best fitting sine-shaped RV curve was computed (see Napiwotzki et al. 2001). The difference between the observed radial velocities and the best fitting theoretical RV curve for each phase set was evaluated in terms of the logarithm of the sum of the squared residuals (χ^2) as a function of period. This method finally results in the data-set's power spectrum which allows to determine the most probable period of variability (see Lorenz et al. 1998).

From the best fit RV curve corresponding to the most probable period, the ephemeris, the system's velocity and the semi-amplitude were derived. As an example, Figure 1 displays the resulting power spectrum and best-fit sine curve for HE 0532−4503. The ephemerides for all program stars, are given in Table 1, as well as the semi-amplitudes (K) and the derived system velocities (γ).

3. QUANTITATIVE SPECTRAL ANALYSIS

Prior to quantitative spectral analysis the spectra were corrected for the measured RV and coadded in order to increase the S/N ratio. Effective temperatures (T_{eff}), surface gravities ($\log g$) and helium abundances ($\log [n_{\mathrm{He}}/n_{\mathrm{H}}]$) were determined by fitting simultaneously each observed hydrogen and helium line with a grid of metal-line blanketed LTE model spectra. The procedure used is described in detail in Napiwotzki et al. (1999). Because of its sensitivity to non-LTE effects, the Hα line was excluded from this analysis. Results are displayed in Table 2, and a sample fit is shown in Figure 2.

In addition, LTE metal abundances were derived for the program stars from measured equivalent widths using the classical curve-of-growth method. Some stars show very rich abundance patterns with many species above the detection threshold (e.g., HE 2135−3749), while others like HE 1448−0510 are extremely metal poor (see also Edelmann 2003). In order to derive upper limits to elemental abundances in these cases, we assumed the detection limit for metal lines to be equal to the S/N level (in terms of equivalent width). Results of our metal abundance analysis are given in Table 3.

4. NATURE OF THE UNSEEN COMPANION

Table 1. System parameters: ephemeris, RV semi-amplitudes K and system velocities γ for all the sdB stars discussed.

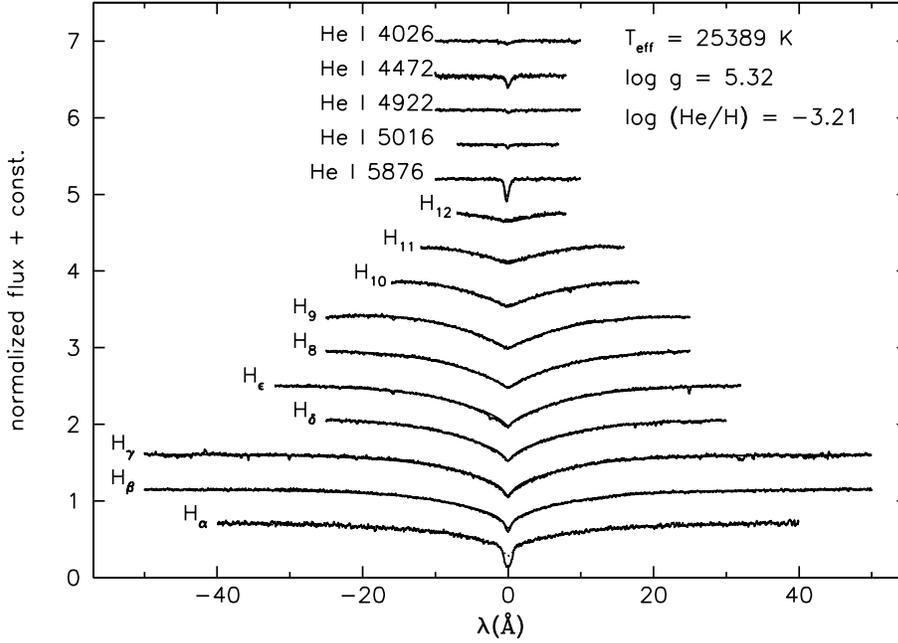| System	Ephemeris [hel.JD$_0$−2 450 000]	K [km s^{-1}]	γ [km s^{-1}]
WD 0048−202	3 097.5596 ± 7.4436 ×E	47.9±0.4	−26.5±0.4
HE 0532−4503	3 099.9975 ± 0.2656 ×E	101.5±0.2	8.5±0.1
HE 0929−0424	3 100.0585 ± 0.4400 ×E	114.3±1.4	41.4±1.0
HE 1448−0510	3 097.0703 ± 7.1588 ×E	53.7±1.1	−45.5±0.8
HE 2135−3749	3 099.6520 ± 0.9240 ×E	90.5±0.6	45.0±0.5
HE 2150−0238	3 100.6081 ± 1.3209 ×E	96.3±1.4	−32.5±0.9

Fig. 2.   Sample model fit for an sdB star (HE 0532-4503) based on 47 UVES spectra.

Since the spectra of the program stars are single-lined, they reveal no information about the orbital motion of the sdBs' companions, and thus we can only compute their mass functions

$$f_{\mathrm{m}} = \frac{M_{\mathrm{comp}}^3 \sin^3 i}{(M_{\mathrm{comp}} + M_{\mathrm{sdB}})^2} = \frac{PK^3}{2\pi G}. \tag{1}$$

Although the RV semi-amplitude K and the period P are determined by the

Table 2. Stellar parameters: effective temperatures, surface gravities and helium abundances of the visible components. Typical error margins for T_{eff}, $\log g$ and $\log[n_{\mathrm{He}}/n_{\mathrm{H}}]$ are 235 K, 0.03 dex and 0.15 dex, respectively.

System	T_{eff} [K]	$\log g$ [cms^{-2}]	$\log[n_{\mathrm{He}}/n_{\mathrm{H}}]$
WD 0048−202	29 960	5.50	≤ −4.00
HE 0532−4503	25 390	5.32	−3.21
HE 0929−0424	29 470	5.71	−1.99
HE 1448−0510	34 690	5.59	−3.06
HE 2135−3749	30 000	5.84	−2.54
HE 2150−0238	30 200	5.83	−2.44

Table 3. Metal abundance patterns of the program stars (relative to solar values).

System	Abundances ϵ					
	C II	N II	O II	Mg II	Al III	Si III
	Si IV	S II	S III	Ar II	Ar III	Ca III
	Ti III	Fe III	Zn III			
WD 0048−202	—	−0.67	−1.38	−1.00	−0.71	−1.50
	−1.98	—	−1.41	—	—	—
	+1.84	−0.27	—			
HE 0532−4503	−2.29	−0.79	−1.17	−0.72	—	−1.22
	—	−0.28	−0.82	—	—	—
	—	0.16	—			
HE 0929−0424	−1.81	−0.14	−1.07	−0.80	−0.53	−0.93
	—	—	−0.80	+0.79	—	—
	—	0.00	—			
HE 1448−0510	$\leq$−2.17	$\leq$−1.24	$\leq$−2.17	−0.59	$\leq$−0.93	—
	—	—	$\leq$+0.80	$\leq$+0.67	—	—
	—	$\leq$−0.46	—			
HE 2135−3749	—	−0.36	—	—	—	—
	—	−0.12	−0.58	+0.74	+0.50	+1.89
	+1.61	−0.87	+1.94			
HE 2150−0238	—	−0.25	$\leq$−2.17	$\leq$−1.53	$\leq$−1.18	$\leq$−2.00
	—	—	−0.26	+0.92	—	—
	—	$\leq$−0.71	—			

RV curve, M_{sdB}, M_{comp} and $\sin^3 i$ remain free parameters. Binary population synthesis models (Han et al. 2003) indicate a most likely mass of $M_{\mathrm{sdB}} = 0.47\,M_\odot$ for sdB stars, which we adopt for the following analysis. Assuming $i = 90°$ we are able to compute the companions' minimum masses from Equation 1. The statistically most probable inclination angle is $i = 52°$ which yields the most likely masses for the companions. Our results are summarized in Table 4.

Table 4. Mass functions, and masses (minimum mass $M_{\mathrm{comp}}^{90°}$ and most probable mass $M_{\mathrm{comp}}^{52°}$) of the unseen companions.

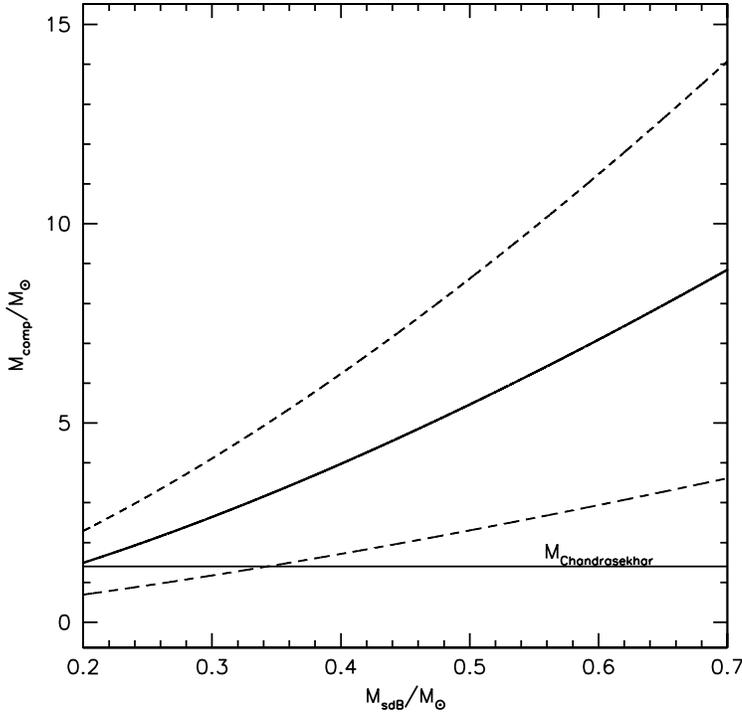| System	f_{m} $[M_\odot]$	$M_{\mathrm{comp}}^{90°}$ $[M_\odot]$	$M_{\mathrm{comp}}^{52°}$ $[M_\odot]$
WD 0048−202	0.085	0.47	0.57
HE 0532−4503	0.029	0.25	0.37
HE 0929−0424	0.068	0.36	0.51
HE 1448−0510	0.115	0.56	0.68
HE 2135−3749	0.071	0.36	0.51
HE 2150−0238	0.122	0.48	0.70

Fig. 3. Determination of the mass of the unseen companion for the system HE 0532-4503. The solid line marks the mean mass for the unseen companion, while the dashed lines indicate the error margins.

5. TIDALLY LOCKED ROTATION?

For close binary systems, rotational velocities of the components may be tidally locked to their orbital motions (see, e.g., Napiwotzki et al. 2001), which means

$$v_{\mathrm{rot}} = \frac{2\pi R_\star}{P}. \tag{2}$$

Measurement of the projected rotational velocities $v_{\mathrm{rot}} \sin i$ would therefore allow to determine inclination angles of the systems, i. In order to derive $v_{\mathrm{rot}} \sin i$, we compared the observed spectra with rotationally broadened synthetic line profiles. The latter ones were computed for the stellar parameters given in Tables 2 and 3. Since sharp metal lines are much more sensitive to rotational broadening than Balmer or helium lines, we concentrated on strong N II lines between 5000 and 5008 Å.

Table 5 displays the resulting projected rotational velocities $v_{\mathrm{rot}} \sin i$, as well as the deduced inclination angles i and corresponding masses M_{comp}. No rotation velocity could be determined for HE 1448−0510 due to the lack of suitable metal lines, the remaining five stars are slow rotators with projected rotational velocities below 10 km s^{-1}. For the short period systems HE 0532−4503, HE 0929−0424 and HE 2135−3749 we deduce inclination angles between 11° and 32°. The analyses of WD 0048−202 and HE 2150−0238, however, yield unreasonable values $\sin i > 1$.

Table 5. Periods and projected rotational velocities, as well as inclination angles and masses of the unseen companion computed for tidally locked rotation.

System	P [d]	R_{sdB} [$R_\odot$]	v_{rot} [km/s]	$v_{rot} \sin i$ [km/s]	i [deg]	M_{comp} [$M_\odot$]
HE 0532−4503	0.2656 ± 0.0001	0.25	47	9 ± 2	11 ± 3	5.0 ± 3.0
HE 0929−0424	0.4400 ± 0.0002	0.16	18	6 ± 2	19 ± 7	2.7 ± 2.0
HE 2135−3749	0.9240 ± 0.0003	0.14	7	4 ± 2	32 ± 20	1.1 ± 0.7
HE 2150−0238	1.3209 ± 0.0050	0.14	—	8 ± 2	$\sin i > 1$	—
HE 1448−0510	7.1588 ± 0.0130	0.18	—	—	—	—
WD 0048−202	7.4436 ± 0.0150	0.20	—	≤ 5	$\sin i > 1$	—

A possible explanation is, that the latter systems are *not* tidally locked, which is plausible because they have rather long periods.

The masses deduced for the companions of the short-period systems are quite large, as can be seen from Table 5. For the HE 2135−3749 system, the sdB companion's mass is 1 $M_\odot$ which indicates a massive white dwarf. The companion of HE 0929−0424 is even more massive, but the large error in mass prevents us from drawing conclusions. For HE 0532−4503 the companion mass is larger than the Chandrasekhar mass, even is we allow for the large error and adopt the canonical mass for the sdB, indicating that it might possibly be a black hole. As can be seen from Figure 3, the companion mass could be sub-Chandrasekhar only if the sdB is of very low mass ($M_{sdB} < 0.34 \, M_\odot$). As indicated by some tests, it will be possible to reduce the uncertainty in $v_{rot} \sin i$ if we include more lines. This will be done in the near future.

Black holes are rare objects and it is therefore very unlikely that our small sample of six RV variable sdBs contain two of them. But stellar rotation and orbital motion may also be locked in a period-ratio that differs from unity (like Mercury, for which the ratio is 3/2).

Since the projected rotational velocities are small, the crucial parameter for the measurement of $v_{rot} \sin i$ and subsequently for M_{comp} is the spectral resolution of the instrument. Our spectra, however, have been measured through rather wide slits. Their spectral resolution is therefore seeing dependent. We used information from the seeing monitor to determine the instrumental profile during these observations. When coadding the spectra we discarded those (few) taken in poor conditions and used only those taken under similar seeing conditions $\sim 1''$. This procedure may have led to an underestimation of the width of the instrumental profile which could have led to an overestimation of the system inclination. A lower inclination means even higher masses. Only if we should still have overestimated the width of the instrumental profile, the companion masses could be lower. To obtain more accurate values for $v_{rot} \sin i$, we need additional observations. These will have to be taken using a small slit so that the instrumental profile is well defined. For the time being the resulting high companion masses have to be taken with a pinch of salt.

REFERENCES

Edelmann H. 2003, Ph.D. thesis, University of Erlangen-Nuremberg

Geier S., Heber U., Przybilla N., Kudritzki R. P. 2006, Baltic Astronomy, 15, 243 (these proceedings)

Han Z., Podsiadlowski P., Maxted P. F. L., Marsh T. R. 2003, MNRAS, 341, 669

Lisker T., Heber U., Napiwotzki R. et al. 2005, A&A, 430, 223

Lorenz L., Mayer P., Drechsel H. 1998, A&A, 332, 909

Maxted P. F. L., Marsh T. R., North R. C. 2000, MNRAS, 317, L41

Napiwotzki R., Christlieb N., Drechsel H. et al. 2003, ESO Messenger, 112, 25

Napiwotzki R., Edelmann H., Heber U. et al. 2001, A&A, 378, L17

Napiwotzki R., Green P. J., Saffer R. A. 1999, ApJ, 517, 399

Napiwotzki R., Karl C., Nelemans G. et al. 2005, in *14th European Workshop on White Dwarfs*, eds. D. Koester & S. Moehler, ASP Conf. Ser., 334, 375